Fractals, Vol. 11, No. 3 (2003) 277–288

World Scientific
www.worldscientific.com

HIDDEN VARIABLE BIVARIATE FRACTAL INTERPOLATION SURFACES

A. K. B. CHAND* and G. P. KAPOOR†
Department of Mathematics, Indian Institute of Technology Kanpur
Kanpur 208016, India
**chand@iitk.ac.in*
†*gp@iitk.ac.in*

Received January 11, 2002
Accepted December 20, 2002

Abstract

We construct hidden variable bivariate fractal interpolation surfaces (FIS). The vector valued iterated function system (IFS) is constructed in $\mathbb{R}^4$ and its projection in $\mathbb{R}^3$ is taken. The extra degree of freedom coming from $\mathbb{R}^4$ provides hidden variable, which is an important factor for flexibility and diversity in the interpolated surface. In the present paper, we construct an IFS that generates both self-similar and non-self-similar FIS simultaneously and show that the hidden variable fractal surface may be self-similar under certain conditions.

Keywords: Bivariate Fractal; Fractal Dimension; FIF; IFS; Surface Generation.

1. INTRODUCTION

Fractal surfaces are currently being given considerable attention due to their applications in areas such as Metallurgy,[1] Earth Sciences,[2,3] Surface Physics,[4,5] Chemistry[6] and Medical Sciences.[7] The approximation of natural surfaces in these areas has emerged as an important research field. Due to complexity of the natural objects, Fractal Geometry is found to be the best tool to approximate these surfaces.

The concept of fractal interpolation function (FIF) was introduced by Barnsley.[8,9] These FIF are self-similar and have fine structure. The construction of univariate hidden variable real-valued FIF, that are not self-similar, has also been discussed by Barnsley.[9,10] P. R. Massopust[11] introduced the construction of fractal surfaces using iterated function system (IFS). The fractal surfaces, using Voss's successive random addition algorithm, have been discussed by Feder.[12] Multiresolution-based fractal

surfaces and their properties have been discussed earlier by Germino et al.[13,14] and Massopust.[15] Xie and Sun[16] constructed bivariate fractal interpolation surfaces (FIS) and discussed their properties.

In the present paper, we introduce hidden variable *bivariate* FIF. The idea is to construct a vector-valued IFS $\{\mathbb{R}^4; W_{n,m}: n = 1, 2, \ldots, N, m = 1, 2, \ldots, M\}$ such that the projection of its attractor G on $\mathbb{R}^3$ is the required interpolation surface. The extra degree of freedom provided by working in $\mathbb{R}^4$ gives us *hidden* variables. These variables may be used to adjust the fractal dimension and shape of the interpolation surfaces. Our construction of IFS is superior to that of Xie and Sun,[16] in the sense that it gives self-similar and non-self-similar FIS simultaneously with the introduction of *constrained free variable* while the construction of Xie and Sun gives only self-similar FIS. The natural projection of attractor G on $\mathbb{R}^3$ gives hidden variable FIS and the projection of G by taking first, second and fourth coordinates simultaneously gives the bivariate FIS as constructed by Xie and Sun.[16] The constrained variable depends on the roughness factor of fractal surface which is generated in the extra degree of freedom. During the study of these surfaces, we find the conditions for coalescence of self-similar surface (FIS) and non-self-similar surface (hidden variable FIS). Since the hidden variable FIS is the projection on $\mathbb{R}^3$ of a fractal in $\mathbb{R}^4$ and it coincides with the fractal surface, in our case the projection of a fractal may be self-similar in nature, in contrast to the observation of Barnsley[9] that the graph of hidden variable FIS is not self-similar, or self-affine, or self-anything.

2. CONSTRUCTION OF HIDDEN VARIABLE BIVARIATE FIS

2.1. Construction of Fractal Surfaces from FIF

Consider the data set $\{(x_i, y_i) \in I \times \mathbb{R}: i = 0, 1, 2, \ldots, N\}$, where $I = [x_0, x_N] \subset \mathbb{R}$. There is a compact subset $K \subset I \times \mathbb{R}$ and a collection of continuous mappings $w_n : K \to K$, $n = 1, 2, \ldots, N$, such that unique attractor of the IFS $\{K; w_n, n = 1, 2, \ldots, N\}$ is the graph G of the FIF f such that $f(x_i) = y_i$, $i = 0, 1, \ldots, N$. The construction, existence and properties of FIF are discussed in the literature.[9,15,17–19] By, translating a FIF along a direction perpendicular to the plane of the function for a distance d, we can get the fractal surface from FIF. This surface can be covered by

$$N(\varepsilon) = \frac{d}{\varepsilon} \times \frac{(x_N - x_0)}{\varepsilon^{\mathcal{D}}} \tag{1}$$

number of small squares of area ε^2, where $\mathcal{D}$ is the fractal dimension of the FIF. The first factor in R.H.S. of Eq. (1) is the number of small squares with side ε along the direction of d and the second factor shows the number of intervals with length ε covering the FIF. It is known that if $\overline{\mathcal{D}}$ is the fractal dimension of this surface, then[20]

$$\overline{\mathcal{D}} = 1 + \mathcal{D} \tag{2}$$

2.2. Principle of Bivariate Hidden Variable FIS

Consider the interpolation data as $\{(x_n, y_m, z_{n,m}) \in R^3 | n = 0, 1, 2, \ldots, N, m = 0, 1, 2, \ldots, M\}$. It is required to construct an interpolation function f: $D \to R$ such that $f(x_n, y_m) = z_{n,m}$ for all $n = 0, 1, 2, \ldots, N$ and $m = 0, 1, 2, \ldots, M$. Consider a generalized set of data as $\{(x_n, y_m, z_{n,m}, t_{n,m}) \in R^4 | n = 0, 1, 2, \ldots, N, m = 0, 1, 2, \ldots, M\}$, where $\{t_{n,m} | n = 0, 1, 2, \ldots, N, m = 0, 1, 2, \ldots, M\}$ is a set of real parameters. Let

$$\begin{aligned} a = x_0 < x_1 < \cdots < x_N = b \\ c = y_0 < y_1 < \cdots < y_M = d \end{aligned} \tag{3}$$

be the partition of $D = I \times J$, $I = [a, b]$, $J = [c, d]$. Set $I_n = [x_{n-1}, x_n]$,

$$J_m = [y_{m-1}, y_m] \quad \text{and} \quad D_{n,m} = I_n \times J_m .$$

Define $\phi_n: I \to I_n$, $\psi_m: J \to J_m$ so that

$$\left.\begin{aligned} \phi_n(x_0) = x_{n-1},\ \phi_n(x_N) = x_n,\ \psi_m(y_0) = y_{m-1},\ \psi_n(y_M) = y_m \\ |\phi_n(c_1) - \phi_n(c_2)| < k_1 |c_1 - c_2|,\ |\psi_m(d_1) - \psi_m(d_2)| < k_2 |d_1 - d_2| \end{aligned}\right\} \tag{4}$$

where $c_1, c_2 \in I$, $d_1, d_2 \in J$, $0 \le k_1 < 1, 0 \le k_2 < 1$.

Define the mapping $L_{n,m}: D \to \mathbb{R}^2$ by $L_{n,m}(x, y) = (\phi_n(x), \psi_m(y))$. It follows that $L_{n,m}$ is a contraction map.

Set $g_1 = \mathrm{Min}_{n,m}\, z_{n,m}$, $g_2 = \mathrm{Max}_{n,m}\, z_{n,m}$, $h_1 = \mathrm{Min}_{n,m}\, t_{n,m}$, $h_2 = \mathrm{Max}_{n,m}\, t_{n,m}$

$\tilde{D} = [g_1, g_2] \times [h_1, h_2]$ and $K = D \times \tilde{D}$. Now, choose $F_{n,m}: K \to \tilde{D}$ to be a continuous function

satisfying

$$\left.\begin{aligned} F_{n,m}(x_0, y_0, z_{0,0}, t_{0,0}) = (z_{n-1,m-1}, t_{n-1,m-1}),\ F_{n,m}(x_N, y_0, z_{N,0}, t_{N,0}) = (z_{n,m-1}, t_{n,m-1}) \\ F_{n,m}(x_0, y_M, z_{0,M}, t_{0,M}) = (z_{n-1,m}, t_{n-1,m}),\ F_{n,m}(x_N, y_M, z_{N,M}, t_{N,M}) = (z_{n,m}, t_{n,m}) \end{aligned}\right\} \tag{5}$$

and

$$d(F_{n,m}(x, y, z, t), F_{n,m}(x^*, y^*, z^*, t^*)) \leq k_3|(z, t) - (z^*, t^*)| \tag{6}$$

for $n \in 1, 2, \ldots, N$, $m \in 1, 2, \ldots, M$, $0 \leq k_3 < 1$, where (x, y, z, t), $(x^*, y^*, z^*, t^*) \in K$ and d is the sup. metric on K.

In the sequel, we use vector valued function $F_{n,m}$ to construct the desired IFS.

2.3. Construction of IFS for Hidden Variable FIS

Let the functions $\phi_n(x) = a_n x + b_n$ and $\psi_m(y) = c_m y + d_m$ satisfy Condition (4).

Then,

$$a_n = \frac{x_n - x_{n-1}}{x_N - x_0}, \quad b_n = \frac{x_{n-1}x_N - x_n x_0}{x_N - x_0}$$

$$c_m = \frac{y_m - y_{m-1}}{y_M - y_0} \quad d_m = \frac{y_{m-1}y_M - y_m y_0}{y_M - y_0}.$$

Hence,

$$\left.\begin{aligned} \phi_n(x) &= x_{n-1} + \frac{x_n - x_{n-1}}{x_N - x_0}(x - x_0) \\ \psi_m(y) &= y_{m-1} + \frac{y_m - y_{m-1}}{y_M - y_0}(y - y_0) \end{aligned}\right\} \tag{7}$$

Now, define,

$$\begin{aligned} F_{n,m}(x, y, z, t) &= (e_{n,m}x + f_{n,m}y + \alpha_{n,m}z + \beta_{n,m}t \\ &\quad + g_{n,m}xy + k_{n,m},\ \tilde{e}_{n,m}x + \tilde{f}_{n,m}y \\ &\quad + \gamma_{n,m}t + \tilde{g}_{n,m}xy + \tilde{k}_{n,m} \end{aligned} \tag{8}$$

Equation (5) gives that

$$\left.\begin{aligned} z_{n-1,m_1} &= e_{n,m}x_0 + f_{n,m}y_0 + \alpha_{n,m}z_{0,0} + \beta_{n,m}t_{0,0} + g_{n,m}x_0y_0 + k_{n,m} \\ z_{n,m_1} &= e_{n,m}x_N + f_{n,m}y_0 + \alpha_{n,m}z_{N,0} + \beta_{n,m}t_{N,0} + g_{n,m}x_Ny_0 + k_{n,m} \\ z_{n-1,m} &= e_{n,m}x_0 + f_{n,m}y_M + \alpha_{n,m}z_{0,M} + \beta_{n,m}t_{0,M} + g_{n,m}x_0y_M + k_{n,m} \\ z_{n,m} &= e_{n,m}x_N + f_{n,m}y_M + \alpha_{n,m}z_{N,M} + \beta_{n,m}t_{N,M} + g_{n,m}x_Ny_M + k_{n,m} \end{aligned}\right\} \tag{9}$$

The system of Eqs. (9) has four equations in six unknowns. Choose $\alpha_{n,m}$ as free variable with $|\alpha_{n,m}| < 1$ and $\beta_{n,m}$ as *constrained free variable* with respect to $\gamma_{n,m}$ such that $|\beta_{n,m}| + |\gamma_{n,m}| < 1$. Consequently,

$$\left.\begin{aligned} g_{n,m} &= \frac{z_{n-1,m-1} - z_{n-1,m} - z_{n,m-1} + z_{n,m} - \alpha_{n,m}(z_{eva}) - \beta_{n,m}(t_{eva})}{x_Ny_M - x_Ny_0 - x_0y_M + x_0y_0} \\ e_{n,m} &= \frac{z_{n-1,m-1} - z_{n,m-1} - \alpha_{n,m}(z_{0,0} - z_{N,0}) - \beta_{n,m}(t_{0,0} - t_{N,0}) - g_{n,m}(x_0y_0 - x_Ny_0)}{x_0 - x_N} \\ f_{n,m} &= \frac{z_{n-1,m-1} - z_{n-1,m} - \alpha_{n,m}(z_{0,0} - z_{0,M}) - \beta_{n,m}(t_{0,0} - t_{0,M}) - g_{n,m}(x_0y_0 - x_0y_M)}{y_0 - y_M} \\ k_{n,m} &= z_{n,m} - e_{n,m}x_N - f_{n,m}y_M - \alpha_{n,m}z_{N,M} - \beta_{n,m}t_{N,M} - g_{n,m}x_Ny_M \end{aligned}\right\} \tag{10}$$

where $z_{eva} = z_{N,M} - z_{N,0} - z_{0,M} + z_{0,0}$ and $t_{eva} = t_{N,M} - t_{N,0} - t_{0,M} + t_{0,0}$.

Similarly, for the second coordinate, we get five unknowns in four equations. Consequently,

$$\left.\begin{aligned} \tilde{g}_{n,m} &= \frac{z_{n-1,m-1} - z_{n-1,m} - z_{n,m-1} + z_{n,m} - \gamma_{n,m}(t_{eva})}{x_Ny_M - x_Ny_0 - x_0y_M + x_0y_0} \\ \tilde{e}_{n,m} &= \frac{z_{n-1,m-1} - z_{n,m-1} - \gamma_{n,m}(t_{0,0} - t_{N,0}) - \tilde{g}_{n,m}(x_0y_0 - x_Ny_0)}{x_0 - x_N} \\ \tilde{f}_{n,m} &= \frac{z_{n-1,m-1} - z_{n-1,m} - \beta_{n,m}(t_{0,0} - t_{0,M}) - \tilde{g}_{n,m}(x_0y_0 - x_0y_M)}{y_0 - y_M} \\ \tilde{k}_{n,m} &= z_{n,m} - \tilde{e}_{n,m}x_N - \tilde{f}_{n,m}y_M - \gamma_{n,m}z_{N,M} - \tilde{g}_{n,m}x_Ny_M \end{aligned}\right\} \tag{11}$$

We wish to construct *Read-Bajraktarević* operator T on the space of vector valued continuous functions from D to $\tilde{D}$. In order to keep the continuity of the image of T on the boundary of $D_{n,m}$, define $G_{n,m}$ in terms of the function $F_{n,m}$ as:

$$G_{n,m}(x, y, z, t) = \begin{cases} F_{n+1,m}(x_0, y, z, t), & x = x_N,\ n = 1, 2, \ldots, N-1,\ m = 1, 2, \ldots, M \\ F_{n,m+1}(x, y_0, z, t), & y = y_M,\ n = 1, 2, \ldots, N,\ m = 1, 2, \ldots, M-1 \\ F_{n,m}(x, y, z, t), & \text{otherwise}. \end{cases} \tag{12}$$

Finally, define the function $W_{n,m}(x, y, z, t)$ on K as:

$$W_{n,m}(x, y, z, t) = (\phi_n(x), \psi_m(y), \quad G_{n,m}(x, y, z, t)) \quad \forall n = 1, 2, \ldots, N \text{ and } m = 1, 2, \ldots, M. \tag{13}$$

Now, $\{\mathbb{R}^4;\ W_{n,m}(x, y, z, t),\ n = 1, 2, \ldots, N,\ m = 1, 2, \ldots, M\}$ is the desired IFS for construction of generalized FIF corresponding to the data $\{(x_n, y_m, z_{n,m}, t_{n,m}) | n = 0, 1, \ldots, N,\ m = 0, 1, \ldots, M\}$ and its projection on $\mathbb{R}^3$ is the hidden variable bivariate FIS.

3. EXISTENCE AND UNIQUENESS OF HIDDEN VARIABLE BIVARIATE FIS

Theorem 1. *Let* $\{\mathbb{R}^4;\ W_{n,m},\ n = 1, 2, \ldots, N,\ m = 1, 2, \ldots, M\}$ *be the IFS defined in Sec.* (2.3) *associated with the data* $\{x_n, y_m, z_{n,m},\ t_{n,m} | n = 0, 1, \ldots, N,\ m = 0, 1, \ldots, M\}$. *Let* $\alpha_{n,m}$, $\beta_{n,m}$ *and* $\gamma_{n,m}$ *in the definition of* $W_{n,m}$ *satisfy* $|\alpha_{n,m}| < 1$, *and* $|\beta_{n,m}| + |\gamma_{n,m}| < 1$ *for all* $n = 1, 2, \ldots, N$, $m = 1, 2, \ldots, M$. *Then there is a metric* τ *on* $\mathbb{R}^4$, *equivalent to the Euclidean metric such that the IFS is hyperbolic with respect to* τ. *In particular, there exists a unique nonempty compact set* $G \subseteq \mathbb{R}^4$ *such that*

$$G = \bigcup_{n=1}^{N} \bigcup_{m=1}^{M} W_{n,m}(G)$$

Proof. Consider the metric τ on $\mathbb{R}^4$ as

$$\tau((x_1, y_1, z_1, t_1), (x_2, y_2, z_2, t_2)) = |x_1 - x_2| + |y_1 - y_2| + \theta(|z_1 - z_2| + |t_1 - t_2|) \tag{14}$$

where θ is to be defined latter.

Then for $x, x^* \neq x_N$, $y, y^* \neq y_M$ and $W_{n,m}$ as in Sec. (2.3),

$$\begin{aligned} &\tau(W_{n,m}(x, y, z, t), W_{n,m}(x^*, y^*, z^*, t^*)) \\ &= |a_n||x - x^*| + |c_m||y - y^*| \\ &\quad + \theta[|e_{n,m}(x - x^*) + f_{n,m}(y - y^*) \\ &\quad + g_{n,m}(xy - x^*y^*) + \alpha_{n,m}(z - z^*) \\ &\quad + \beta_{n,m}(t - t^*)| + |\tilde{e}_{n,m}(x - x^*) + \tilde{f}_{n,m}(y - y^*) \\ &\quad + \tilde{g}_{n,m}(xy - x^*y^*) + \gamma_{n,m}(t - t^*)|] \\ &\leq (|a_n| + \theta(|e_{n,m}| + |\tilde{e}_{n,m}|))|x - x^*| \\ &\quad + (|c_m| + \theta(|f_{n,m}| + |\tilde{f}_{n,m}|))|y - y^*| \\ &\quad + \theta(|g_{n,m}| + |\tilde{g}_{n,m}|)|x(y - y^*) + y^*(x - x^*)| \\ &\quad + \theta(|\alpha_{n,m}||z - z^*| + (|\beta_{n,m}| + |\gamma_{n,m}|)|t - t^*|) \\ &\leq (|a_n| + \theta(|e_{n,m}| + |\tilde{e}_{n,m}| \\ &\quad + |g_{n,m}y_M| + |\tilde{g}_{n,m}y_M|)|x - x^*| \\ &\quad + (|c_m| + \theta(|f_{n,m}| + |\tilde{f}_{n,m}| + |g_{n,m}x_N| \\ &\quad + |\tilde{g}_{n,m}x_N|)|y - y^*| + \theta(|\alpha_{n,m}||z - z^*| \\ &\quad + (|\beta_{n,m}| + |\gamma_{n,m}|)|t - t^*|) \end{aligned} \tag{15}$$

Now set,

$$\theta_1 = \frac{\min_{1 \leq n \leq N}(1 - |a_n|)}{\max_{1 \leq n \leq N,\ 1 \leq m \leq M} 2\{|e_{n,m}| + |\tilde{e}_{n,m}| + |g_{n,m}y_M| + |\tilde{g}_{n,m}y_M|\}}$$

$$\theta_2 = \frac{\min_{1 \leq m \leq M}(1 - |c_m|)}{\max_{1 \leq n \leq N,\ 1 \leq m \leq M} 2\{|f_{n,m}| + |\tilde{f}_{n,m}| + |g_{n,m}x_N| + |\tilde{g}_{n,m}x_N|\}}$$

and define $\theta = \min(\theta_1, \theta_2)$. With this definition of θ, the Inequality (15) gives $\tau(W_{n,m}(x, y, z, t), W_{n,m}(x^*, y^*, z^*, t^*))$

$$\leq \frac{(1+|a_n|)}{2}|x-x^*| + \frac{(1+|c_m|)}{2}|y-y^*| + \theta\delta(|z-z^*|+|t-t^*|)$$
$$< s(|x-x^*|+|y-y^*|+\theta(|z-z^*|+|t-t^*|))$$

where

$$s = \max\left\{\frac{(1+|a_n|)}{2}(1 \leq n \leq N), \frac{(1+|c_m|)}{2}(1 \leq m \leq M), \delta\right\} < 1$$

and

$$\delta = \max_{1\leq n\leq N,\, 1\leq m\leq M}\{|\alpha_{n,m}|, |\beta_{n,m}| + |\gamma_{n,m}|\} < 1.$$

For x, $x^* = x_N$ or y, $y^* = y_M$, the proof follows the same steps by defining suitable θ. Hence, $W_{n,m}$'s are hyperbolic in nature. It follows now, by fixed point theorem, there exists a unique nonempty compact set $G \subset \mathbb{R}^4$ such that $G = \bigcup_{n=1}^{N}\bigcup_{m=1}^{M} W_{n,m}(G)$. □

Theorem 2. *Let G be the attractor of the IFS defined in Theorem* 1. *Then, G is the graph of the continuous vector valued function $F : D \to \tilde{D}$ such that $F(x_n, y_m) = (z_{n,m}, t_{n,m})$ for all $n = 1, 2, \ldots, N$; $m = 1, 2, \ldots, M$. i.e. $G = \{(x, y, z(x, y), t(x, y) | (x, y) \in D\}$ and D, $\tilde{D}$ are defined as in Sec* (2.2).

Proof. Consider the family of functions,

$$\mathcal{F} = \{F : D \to \tilde{D} | F \text{ is continuous}, F(x_0, y_0) = (z_{0,0}, t_{0,0}), F(x_N, y_0) = (z_{N,0}, t_{N,0}), F(x_0, y_M) = (z_{0,M}, t_{0,M}), F(x_N, y_M) = (z_{N,M}, t_{N,M})\}$$

For $F, \tilde{F} \in \mathcal{F}$, define the metric $\rho(F, \tilde{F}) = \sup_{(x,y)\in D} \|F(x, y) - \tilde{F}(x, y)\|$ where $\|\cdot\|$ denotes the norm on $\mathbb{R}^2$. Then $(\mathcal{F}, \rho)$ is a complete metric space.

Now, for all $(x, y) \in D_{n,m}$, define *Read-Bajraktarević* operator T on $(\mathcal{F}, \rho)$ as

$$(TF)(x, y) = G_{n,m}(\phi_n^{-1}(x), \psi_m^{-1}(y), z((\phi_n^{-1}(x), \psi_m^{-1}(y)), t((\phi_n^{-1}(x), \psi_m^{-1}(y))) \quad (16)$$

We prove first in the sequel that T maps $\mathcal{F}$ into itself.

For $F \in \mathcal{F}$,

$$\begin{aligned}(TF)(x_0, y_0) &= G_{1,1}(\phi_1^{-1}(x_0), \psi_1^{-1}(y_0), z((\phi_1^{-1}(x_0), \psi_1^{-1}(y_0)), t((\phi_1^{-1}(x_0), \psi_1^{-1}(y_0)))\\ &= G_{1,1}(x_0, y_0, z_{0,0}, t_{0,0})\\ &= F_{1,1}(x_0, y_0, z_{0,0}, t_{0,0})\\ &= (z_{0,0}, t_{0,0})\end{aligned}$$

Similarly,

$$\begin{aligned}(TF)(x_N, y_0) &= (z_{N,0}, t_{N,0}), (TF)(x_0, y_M)\\ &= (z_{0,M}, t_{0,M}), \text{ and } (TF)(x_N, y_M)\\ &= (z_{N,M}, t_{N,M})\end{aligned}$$

With A_1, A_2, A_3, A_4 as in Fig. 1, by the definition of TF,

$$\begin{aligned}\lim_{\substack{(x,y)\to(x_n,y_m)\\(x,y)\in A_1}}(TF)(x, y) &= \lim_{\substack{(x,y)\to(x_n,y_m)\\(x,y)\in A_2}}(TF)(x, y)\\ &= \lim_{\substack{(x,y)\to(x_n,y_m)\\(x,y)\in A_3}}(TF)(x, y)\\ &= \lim_{\substack{(x,y)\to(x_n,y_m)\\(x,y)\in A_4}}(TF)(x, y)\\ &= (z_{n,m}, t_{n,m})\end{aligned}$$

where $n = 1, 2, \ldots, N-1$; $m = 1, 2, \ldots, M-1$. Also, for $\overline{y} \in [y_m, y_m - 1]$,

$$\begin{aligned}&\lim_{\substack{(x,y)\to(x_n,\overline{y})\\(x,y)\in A_3}}(TF)(x, y)\\ &= F_{n+1,m+1}(x_0, \psi_{m+1}^{-1}\overline{y}, z(x_0, \psi_{m+1}^{-1}\overline{y}), t(x_0, \psi_{m+1}^{-1}\overline{y}))\\ &= \lim_{\substack{(x,y)\to(x_n,\overline{y})\\(x,y)\in A_4}}(TF)(x, y)\end{aligned}$$

Similarly, for all n and m, TF is continuous on boundaries of $D_{n,m}$. Consequently, $TF \in \mathcal{F}$. □

Next, we prove that T is a contraction map on $\mathcal{F}$. For $F \in \mathcal{F}$, define $z_F(x, y)$, $t_F(x, y)$ as z-value and t-value of the vector valued function TF at the point (x, y). Let F, $H \in \mathcal{F}$ and $(x, y) \in D_{n,m}$, then

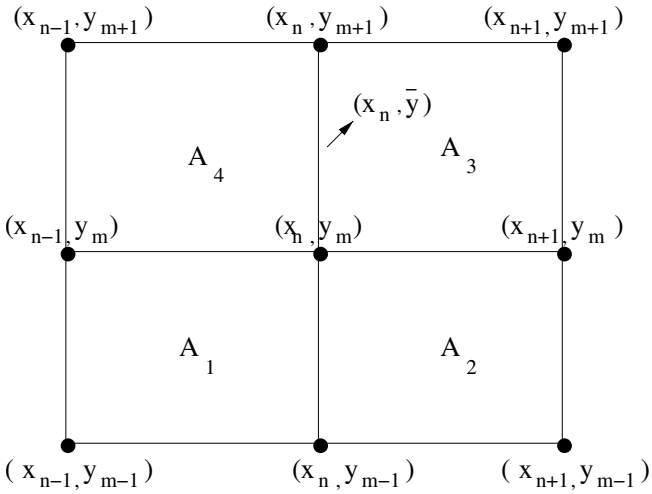

Fig. 1 Continuity domains of TF.

$$
\begin{aligned}
&\rho(TF, TH)\\
&\quad = \sup_{(x,y)\in D}\{\|TF(x,y) - TH(x,y)\|\}\\
&\quad = \sup_{(x,y)\in D}\{\|\alpha_{n,m}(z_F(\phi_n^{-1}(x),\, \psi_m^{-1}(y))\\
&\qquad - z_H(\phi_n^{-1}(x)), \psi_m^{-1}(y))) + \beta_{n,m}(t_F(\phi_n^{-1}(x)\,,\\
&\qquad \psi_m^{-1}(y)) - t_H(\phi_n^{-1}(x), \psi_m^{-1}(y)))\,,\\
&\qquad \gamma_{n,m}(t_F(\phi_n^{-1}(x),\, \psi_m^{-1}(y)) - t_H(\phi_n^{-1}(x)\,,\\
&\qquad \psi_m^{-1}(y)))\|\}\\
&\quad \le \delta_{(x,y)\in D}\sup\{\|z_F(\phi_n^{-1}(x), \psi_m^{-1}(y))\\
&\qquad - z_H(\phi_n^{-1}(x), \psi_m^{-1}(y)) + t_F(\phi_n^{-1}(x), \psi_m^{-1}(y))\\
&\qquad - t_H(\phi_n^{-1}(x), \psi_m^{-1}(y)),\, t_F(\phi_n^{-1}(x)\,,\\
&\qquad \psi_m^{-1}(y)) - t_H(\phi_n^{-1}(x), \psi_m^{-1}(y))\|\}\\
&\quad \le \delta\rho(F, H)
\end{aligned}
$$

where in view of the condition on $\alpha_{n,m}$, $\beta_{n,m}$, $\gamma_{n,m}$ imposed in Theorem 1,

$$\delta = \max_{1\le n\le N, 1\le m\le M}\{|\alpha_{n,m}|,\, |\beta_{n,m}|,\, |\gamma_{n,m}|\} < 1\,.$$

This establishes that T is a contraction mapping. By fixed point theorem, T has a fixed point, i.e. there exists a vector valued function $F_0 \in \mathcal{F}$ such that for all $(x, y) \in D$, $(TF_0)(x, y) = F_0(x, y) = (z_0(x, y), t_0(x, y))$. Now, for all $n \in 0, 1, \ldots, N$, $m \in 0, 1, \ldots, M$,

$$
\begin{aligned}
F_0(x_n, y_m) &= (TF_0)(x_n, y_m)\\
&= G_{n+1,m+1}(\phi_{n+1}^{-1}(x_n),\, \psi_{m+1}^{-1}(y_m),\\
&\quad F_0(\phi_{n+1}^{-1}(x_n),\, \psi_{m+1}^{-1}(y_m))\\
&= F_{n+1,m+1}(x_0,\, y_0,\, z_{0,0},\, t_{0,0})\\
&= (z_n,\, t_m)
\end{aligned}
$$

This establishes that F_0 is the function which interpolates the data $\{(x_n, y_m, z_{n,m}, t_{n,m}) | n = 0, 1, \ldots, N, m = 0, 1, \ldots, M\}$.

It remains to show that the graph $\tilde{G}$ of the vector valued function F_0 is the attractor of the IFS defined in Theorem 1. To this end observe that for all $(x, y) \in D$, $n = 1, 2, \ldots, N$, $m = 1, 2, \ldots, M$ and for all $F \in \mathcal{F}$,

$$
\begin{aligned}
(TF)(\phi_n(x),\, \psi_m(y)) &= F_{n,m}(x,\, y,\, z(x,\, y),\, t(x,\, y))\\
&= F_{n,m}(x,\, y,\, z(x,\, y),\, t(x,\, y))\\
&= (e_{n,m}x + f_{n,m}y + \alpha_{n,m}z\\
&\quad + \beta_{n,m}t + g_{n,m}xy\\
&\quad + k_{n,m},\, \tilde{e}_{n,m}x + \tilde{f}_{n,m}y\\
&\quad + \gamma_{n,m}t + \tilde{g}_{n,m}xy + \tilde{k}_{n,m})
\end{aligned}
$$

Also,

$$
\begin{aligned}
W_{n,m}\begin{pmatrix} x\\ y\\ z(x,\, y)\\ t(x,\, y)\end{pmatrix} &= \begin{pmatrix} \phi_n(x)\\ \psi_m(y)\\ G_{n,m}(x,\, y,\, z,\, t)\end{pmatrix}\\
&= \begin{pmatrix} \phi_n(x)\\ \psi_m(y)\\ TF_0(\phi_n(x), \psi_m(y))\end{pmatrix}\\
&= \begin{pmatrix} \phi_n(x)\\ \psi_m(y)\\ F_0(\phi_n(x),\, \psi_m(y))\end{pmatrix}
\end{aligned}
$$

which shows that $\tilde{G}$ satisfies the invariance property, i.e.

$$\tilde{G} = \bigcup_{n=1}^{N}\bigcup_{m=1}^{M} W_{n,m}(\tilde{G})$$

However, by Theorem 1, the nonempty compact set that satisfies the invariance property is unique. Consequently, $G = \tilde{G}$. This proves that G is the graph of the vector valued function F_0 such that $G = \{(x, y, F_0(x, y) | (x, y) \in D\}$.

Remark 3. The surface obtained as the projection of G on $\mathbb{R}^3$ is described by $\{(x, y, z(x, y): (x, y) \in D\}$ and is called *hidden variable FIS* for

the given interpolation data $\{(x_n, y_m, z_{n,m})|n = 0, 1, \ldots, N, m = 0, 1, \ldots, M\}$.

For a given set of bivariate surface data, if we add an extra dimension to construct hidden variable linear FIS, then we have one free variable in the fourth coordinate whereas, in the third coordinate, we have one free variable and one constrained variable. In the case $z_{n,m} = t_{n,m}$, the resulting scaling factor of hidden variable FIS is $\alpha_{n,m} + \beta_{n,m}$. As $|\alpha_{n,m}| < 1$ and $|\beta_{n,m}| + |\gamma_{n,m}| < 1$, taking $|\gamma_{n,m}| < \varepsilon$ for sufficiently small ε, the scaling factor of hidden variable FIS lies between -2^+ and 2^-. Inductively, if extra n-dimensions are added to bivariate surface data, $(n+3)$th coordinate has one free variable to get interpolated fractal surface, $(n+2)$th coordinate has one free variable and may have at most one constrained free variable, $(n+1)$th coordinate has one free variable and may have at most two constrained free variables, ... Continuing, the third coordinate has one free variable and may have at most n constrained free variables. So, in this extension, there are n free variables and at most $(1+2+3+\cdots+n)$ free variables in the hidden variable FIS. Due to the restrictions on free variables and constrained free variables, the scaling factor of hidden variable FIS lies between $-(n+1)^+$ and $(n+1)^-$. Thus, one can expect a wide ranges of hidden variable FIS in the higher dimension extensions.

4. EXAMPLES AND RESULTS

Consider the interpolation data as in Table 1. There are nine data points on the surface. The linear surface from this data is drawn in Fig. 2. The generated hidden variable FIS from the data in Table 1 with $\alpha_{n,m} = 0.7$, $\beta_{n,m} = 0.4$ and $\gamma_{n,m} = 0.3$ is shown in Fig. 3. Figures 4 to 7 give different hidden variable FIS generated with different values of $\alpha_{n,m}$, $\beta_{n,m}$ and $\gamma_{n,m}$.

For a given surface, define its average roughness as $R_a = \sum_{n,m} z_{n,m} / \sum_{n,m} 1$. The average roughness of linear surface in Fig. 2 is 0.53125. The noise N of any generated surface with respect to linear surface is defined as the ratio of their average roughnesses. The variance V of $z_{n,m}$'s of any generated surface describes the distribution of z-values on that surface and so gives the information about roughness of the surface. The variance of z-values for the linear surface in Fig. 2 is 0.0061. The root mean square roughness R_q of any generated surface with respect

Table 1 Interpolation data.

Y \ X	**1**	**2**	**3**
1	0.3 *0.3*	0.7 *0.7*	0.8 *0.6*
2	0.5 *0.4*	0.4 *0.8*	0.5 *0.8*
3	0.6 *0.5*	0.6 *0.5*	0.6 *0.9*

Data points on the top left corner of a box $\equiv z_{n,m}$.
Data points on the bottom right corner of a box $\equiv t_{n,m}$.

to linear surface is defined as

$$R_q = \sqrt{\sum_{n,m} (z_{n,m} - z^*_{n,m})^2}$$

where the $z_{n,m}$'s are z-values on the generated surfaces and $z^*_{n,m}$'s are z-values of the linear surface. The calculated values of R_a, N, V and R_q for the

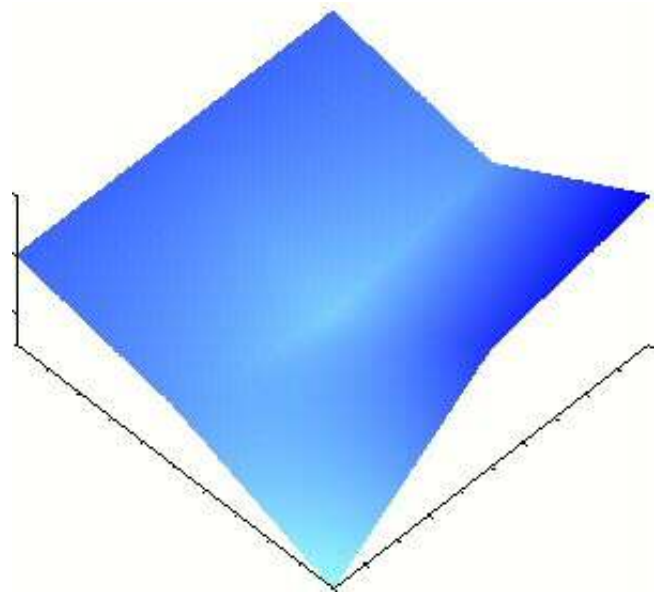

Fig. 2 Linear surface from original data.

Table 2 Average roughness (Ra), noise (N), variance (V) and root mean square roughness (Rq) for the generated interpolation surfaces in Figs. 2 to 13.

Details of Figures	Average Roughness ($\mathbf{R_a}$)	Noise (N)	Variance of $\mathbf{Z_{n,m}(V)}$	Root Mean Square Roughness ($\mathbf{R_q}$)
Fig 2 linear surface from interpolation data as in Table 1.	0.53125	1.00	0.0061	0.0
Fig 3 Hidden variable FIS with $\alpha_{n,m} = 0.7$, $\beta_{n,m} = 0.4$, $\gamma_{n,m} = 0.3$ and $t_{n,m}$ as in Table 1.	0.701441	1.32	0.0117144	36.4398
Fig. 4 Hidden variable FIS with $\alpha_{n,m} = 0.9$, $\beta_{n,m} = 0.4$, $\gamma_{n,m} = 0.3$ and $t_{n,m}$ as in Table 1.	0.833173	1.568	0.029371	60.1616
Fig. 5 Hidden variable FIS with $\alpha_{n,m} = 0.7$, $\beta_{n,m} = 0.6$, $\gamma_{n,m} = 0.3$ and $t_{n,m}$ as in Table 1.	0.792524	1.492	0.0175995	53.4664
Fig. 6 Hidden variable FIS with $\alpha_{n,m} = 0.5$, $\beta_{n,m} = 0.6$, $\gamma_{n,m} = 0.3$ and $t_{n,m}$ as in Table 1.	0.697358	1.313	0.0110018	36.18
Fig. 7 Hidden variable FIS with $\alpha_{n,m} = 0.7$, $\beta_{n,m} = 0.4$, $\gamma_{n,m} = 0.5$ and $t_{n,m}$ as in Table 1.	0.765991	1.442	0.0143968	47.0527
Fig. 8 Hidden variable FIS with parameters as in Fig. 3, with $t_{0,0} = 3$, $t_{0,1} = 4$, $t_{0,2} = 1$, $t_{1,0} = 6$, $t_{1,1} = 7$, $t_{1,2} = 5$, $t_{2,0} = 9$, $t_{2,1} = 8$, $t_{2,2} = 2$.	2.90634	5.471	0.382988	447.626
Fig. 9 Hidden variable FIS with $\alpha_{n,m} = 0.9$, $\beta_{n,m} = -0.25$, $\gamma_{n,m} = 0.7$ and with $t_{n,m} = z_{n,m}$.	0.516886	0.973	0.00671278	11.203
Fig. 10 Fractal surface with $\gamma_{n,m} = 0.7$ from the same IFS for Fig. 9 by taking 1st, 2nd and 4th co-ordinates.	0.519274	0.977	0.0076889	13.3355
Fig. 11 Coalescence surface with $\alpha_{n,m} = 0.7$, $\beta_{n,m} = -0.2$, $\gamma_{n,m} = 0.5$ and $t_{n,m} = z_{n,m}$.	0.520932	0.98	0.00586607	7.8643
Fig. 12 Hidden variable FIS with $\alpha_{n,m} = 0.9$, $\beta_{n,m} = 0.9$, $\gamma_{n,m} = 0.05$ and $t_{n,m} = z_{n,m}$.	0.527274	0.992	0.0667239	50.8205
Fig. 13 Hidden variable FIS with $\alpha_{n,m} = -0.9$, $\beta_{n,m} = -0.9$, $\gamma_{n,m} = 0.05$ and $t_{n,m} = z_{n,m}$.	0.536457	1.01	0.0596593	44.2678

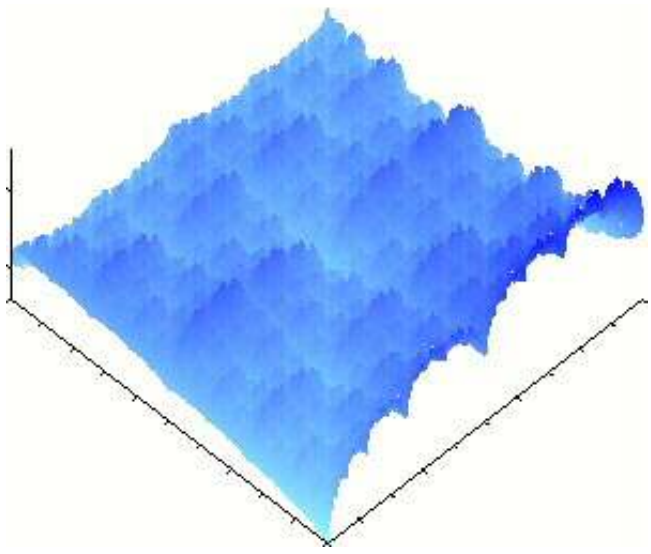

Fig. 3 Hidden variable FIS with $\alpha_{n,m} = 0.7$, $\beta_{n,m} = 0.4$, $\gamma_{n,m} = 0.3$ and $t_{n,m}$ as in Table 1.

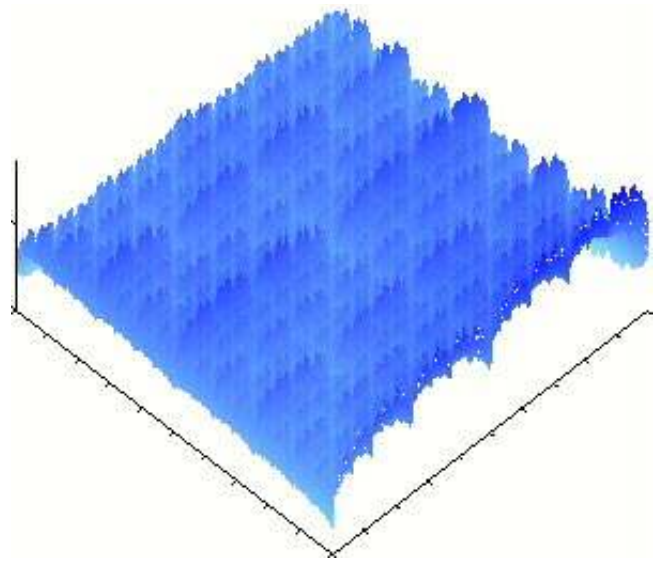

Fig. 4 Effect of change in $\alpha_{n,m}$ on hidden variable FIS with $\alpha_{n,m} = 0.9$, $\beta_{n,m} = 0.4$, $\gamma_{n,m} = 0.3$ and $t_{n,m}$ as in Table 1.

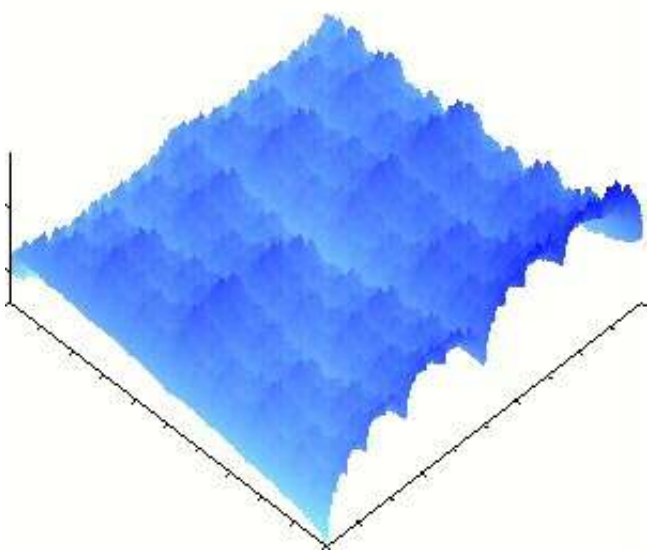

Fig. 5 Effect of change in $\beta_{n,m}$ on hidden variable FIS with $\alpha_{n,m} = 0.7$, $\beta_{n,m} = 0.6$, $\gamma_{n,m} = 0.3$ and $t_{n,m}$ as in Table 1.

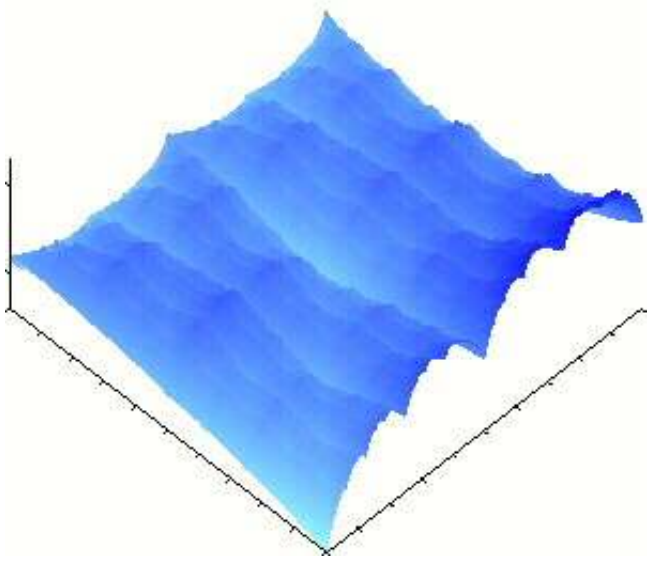

Fig. 6 Effect of change in $\alpha_{n,m}$ and $\beta_{n,m}$ on hidden variable FIS with $\alpha_{n,m} = 0.5$, $\beta_{n,m} = 0.6$, $\gamma_{n,m} = 0.3$ and $t_{n,m}$ as in Table 1.

generated surfaces in Figs. 3 to 13 are given in Table 2.

On comparison with linear surface in Fig. 2, the effect of change in the values of $\alpha_{n,m}$, $\beta_{n,m}$ and $\gamma_{n,m}$ on hidden variable FIS can easily be seen with the help of Table 2. Figure 3 is the hidden variable FIS with $R_a = 0.701441$, $N = 1.32$, $V = 0.0117144$ and $R_q = 36.4398$. The hidden variable FIS generated in Fig. 4 with an increase in the values of $\alpha_{n,m}$ by 0.2 shows that all the values of the roughness parameters R_a, N, V and R_q increase in this case.

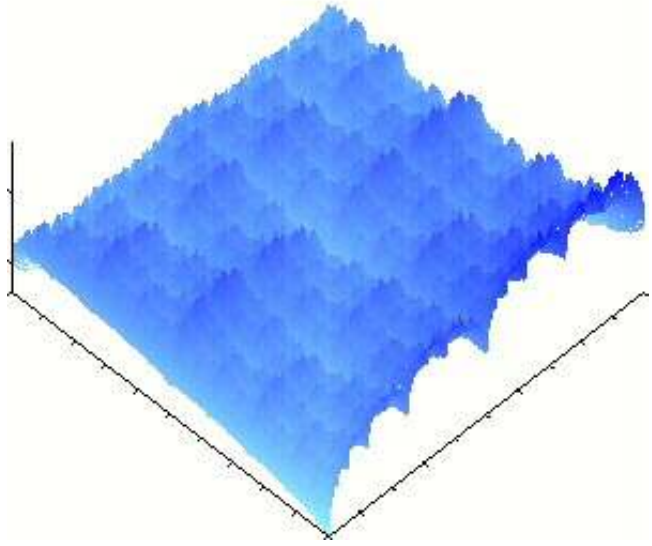

Fig. 7 Effect of change in $\gamma_{n,m}$ on hidden variable FIS with $\alpha_{n,m} = 0.7$, $\beta_{n,m} = 0.4$, $\gamma_{n,m} = 0.5$ and $t_{n,m}$ as in Table 1.

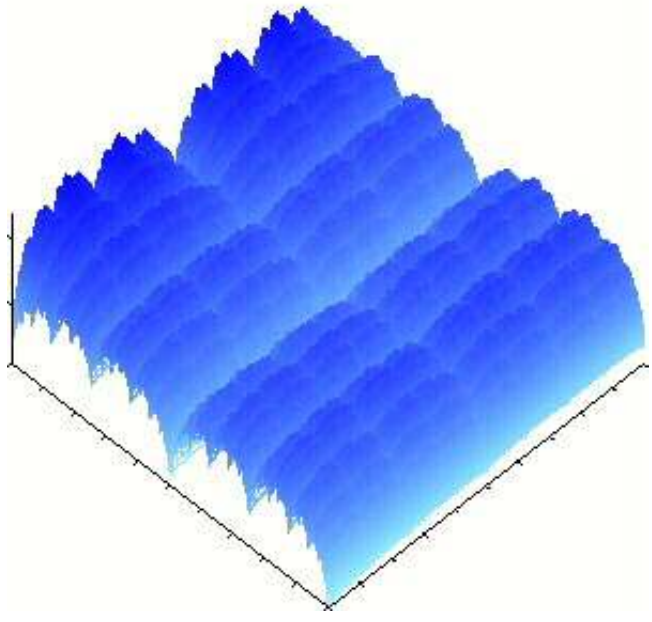

Fig. 8 Hidden variable FIS with same parameter as in Fig. 3, with $\{t_{0,0} = 3, t_{0,1} = 4, t_{0,2} = 1, t_{1,0} = 6, t_{1,1} = 7, t_{1,2} = 5, t_{2,0} = 9, t_{2,1} = 8, t_{2,2} = 2\}$.

Thus, the greater the value of $\alpha_{n,m}$, the more irregular is the surface in nature. The hidden variable FIS generated in Fig. 5 with an increase in the value of $\beta_{n,m}$ by 0.2 again demonstrates that all the values of roughness parameter increase but this increase is lesser in comparison to generated FIS in Fig. 4. However, equal variations in $\alpha_{n,m}$ (with fixed values of $\beta_{n,m}$, $\gamma_{n,m}$) and $\beta_{n,m}$ (with fixed values of $\alpha_{n,m}$, $\gamma_{n,m}$) result in different structure of

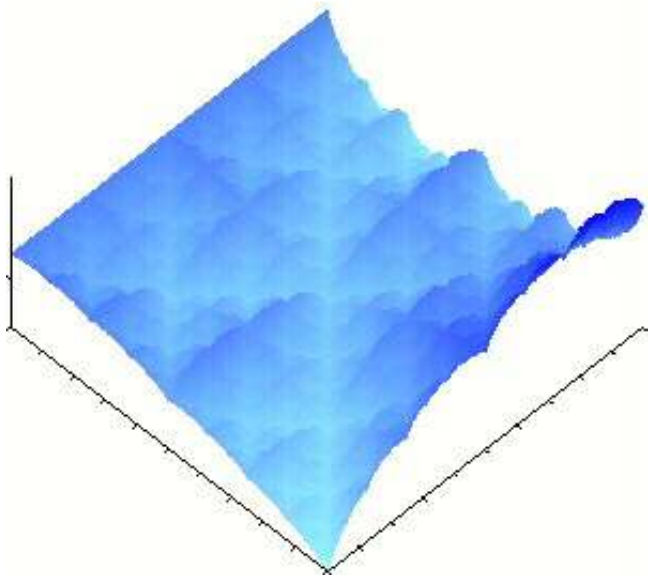

Fig. 9 Hidden variable FIS with $\alpha_{n,m} = 0.9$, $\beta_{n,m} = -0.25$, $\gamma_{n,m} = 0.7$ when $t_{n,m} = z_{n,m}$.

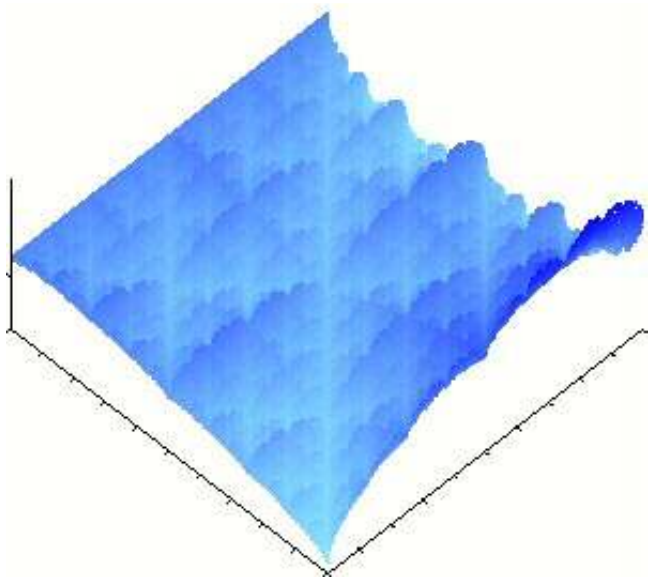

Fig. 10 Fractal surface with $\gamma_{n,m} = 0.7$ from same algorithm.

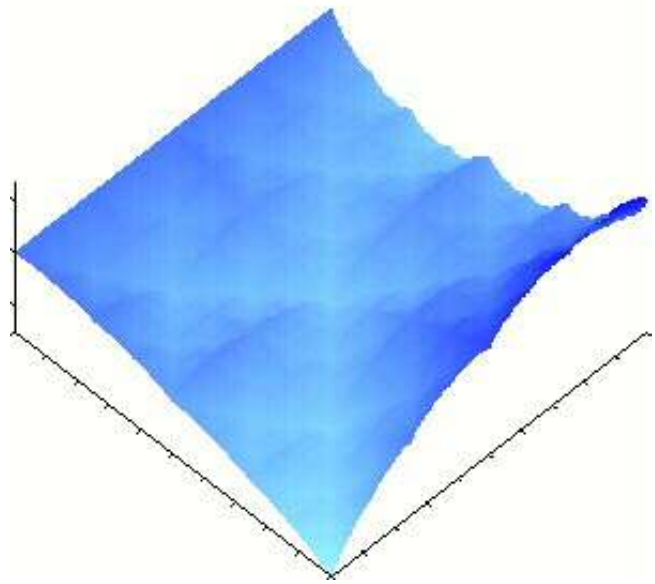

Fig. 11 Coalescence surface with $\alpha_{n,m} = 0.7$, $\beta_{n,m} = -0.2$, $\gamma_{n,m} = 0.5$.

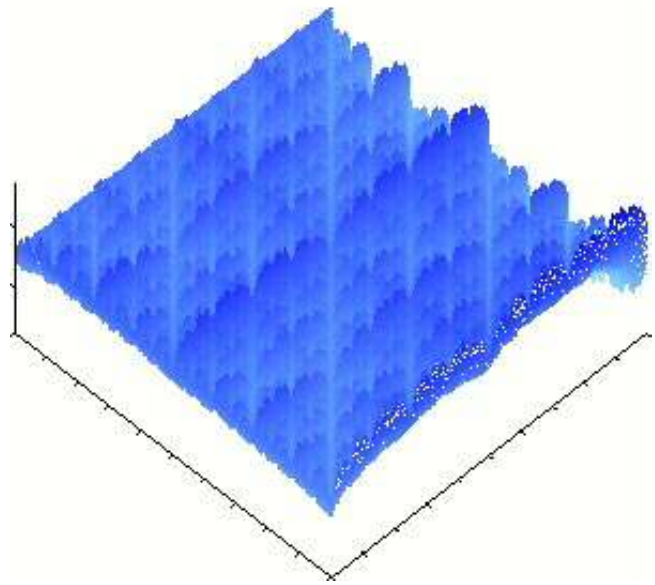

Fig. 12 Hidden variable FIS with $\alpha_{n,m} = 0.9$, $\beta_{n,m} = 0.9$, $\gamma_{n,m} = 0.05$ when $t_{n,m} = z_{n,m}$.

hidden variable FIS. The hidden variable FIS in Fig. 6 is generated with different values of $\alpha_{n,m}$ and $\beta_{n,m}$. Although in both Figs. 3 and 6, $\alpha_{n,m}+\beta_{n,m} = 1.1$, their structures are completely different. Thus, the variation of roughness parameters vary according to the magnitudes of $\alpha_{n,m}$ and $\beta_{n,m}$.

The hidden variable FIS in Fig. 7 is generated with an increase in the value of $\gamma_{n,m}$ by 0.2. The hidden variable $\gamma_{n,m}$ has least effect on the structure of hidden variable FIS, when compared with R_a, N, V and R_q of hidden variable FISs with same amount of variations in $\alpha_{n,m}$ or $\beta_{n,m}$. Therefore, it can be used to simulate any complex geometrical structure once we fix $\alpha_{n,m}$, $\beta_{n,m}$ and $t_{n,m}$.

Figure 8 shows a hidden variable FIS generated for a new set of $t_{n,m}$ as $\{t_{0,0} = 3, t_{0,1} = 4, t_{0,2} = 1, t_{1,0} = 6, t_{1,1} = 7, t_{1,2} = 5, t_{2,0} = 9, t_{2,1} = 8, t_{2,2} = 2\}$ and the same set of values for $\alpha_{n,m}$, $\beta_{n,m}$ and $\gamma_{n,m}$ as in Fig. 3. It is found that the values

of $t_{n,m}$'s can change the structure of interpolation surface in arbitrary manner as the magnitude of R_a, N, V and R_q depend on the magnitude of this extra-dimensional value of $t_{n,m}$'s.

As a last case, we consider $t_{n,m} = z_{n,m}$ in Figs. 9 to 13. For $\alpha_{n,m} = 0.9$, $\beta_{n,m} = -0.25$ and $\gamma_{n,m} = 0.7$, the hidden variable FIS $\Gamma = \{(x, y, z(x, y)|(x, y) \in D\}$ and FIS $\Gamma^* = \{(x, y, t(x, y)|(x, y) \in D = \tilde{D}\}$ are given in Figs. 9 and 10 respectively. From Table 2, these surfaces are not too much irregular in these cases. When $\alpha_{n,m} + \beta_{n,m} = \gamma_{n,m}$ with $z_{n,m} = t_{n,m}$, the hidden variable FIS Γ and FIS Γ^* coincide. For $\alpha_{n,m} = 0.7$, $\beta_{n,m} = -0.2$ and $\gamma_{n,m} = 0.5$, the coalesced fractal surface is shown in Fig. 11. From Table 2, it is found that V and R_q are minimum for coalesced surface compared with other hidden variable FIS. For $\alpha_{n,m} = \pm 0.9$, $\beta_{n,m} = \pm 0.9$ and $\gamma_{n,m} = 0.05$, the scaling factor of hidden variable surface lies between -2^+ and 2^-. The hidden variable FIS constructed in this case are given in Figs. 12 and 13, respectively. From Table 2, it is found that the surfaces are very irregular in shape when the magnitude of resulting scaling factor is close to 2. Since, the values of V and R_q are high when the resulting scaling factor tends to 2^- or -2^+ for one-dimensional extension, one can expect higher values of V and R_q in the higher dimension extension when the resulting scaling factor tends to $-(n+1)^+$ or $(n+1)^-$.

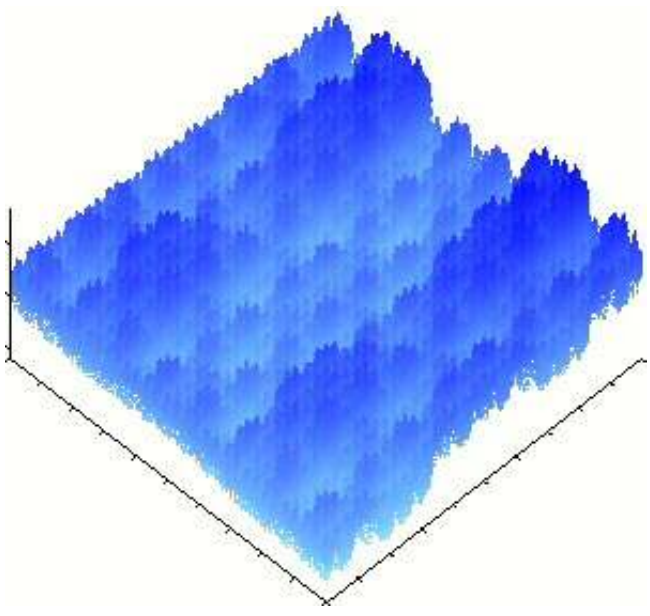

Fig. 13 Hidden variable FIS with $\alpha_{n,m} = -0.9$, $\beta_{n,m} = -0.9$, $\gamma_{n,m} = 0.05$ when $t_{n,m} = z_{n,m}$.

5. CONCLUSION

Using the concept of constrained free variable introduced here, an IFS is constructed for generating hidden variable FIS. The existence and uniqueness of hidden variable FIS is proved by choosing suitable values of $\alpha_{n,m}$, $\beta_{n,m}$ and $\gamma_{n,m}$, and extra coordinate $t_{n,m}$. The variable $\gamma_{n,m}$ is used to simulate a wide range of surfaces for different values of $\alpha_{n,m}$, $\beta_{n,m}$, $t_{n,m}$, $|\gamma_{n,m}| \leq 1 - |\beta_{n,m}|$. The effect of change in $\alpha_{n,m}$, $\beta_{n,m}$, $\gamma_{n,m}$ and $t_{n,m}$ on the roughness of surface is also studied. Our IFS gives both self-similar surfaces Γ and non-self-similar surfaces Γ^* simultaneously, whereas the construction of Xie and Sun[16] gives only self-similar FIS.

If we construct hidden variable fractal surfaces by increasing n-dimensions linearly to any set of interpolation data in $\mathbb{R}^3$, we can choose $(n+1)$ *free variables* and at most $(1 + 2 + \cdots + n)$ *constrained free variables*. If all extra n-dimensions take the same values of $z_{n,m}$, the scaling factor of hidden variable surfaces lies between $-(n+1)^+$ and $(n+1)^-$.

There is no formula in closed form for finding fractal dimension of hidden variable FIS. However, when hidden variable FIS coincides with fractal surface, the fractal dimension can easily be calculated by finding the fractal dimension of coalesced fractal surface. We have not considered here the effect of change in $\alpha_{n,m}$, $\beta_{n,m}$, $\gamma_{n,m}$ and $t_{n,m}$ on the fractal dimension of general hidden variable FIS. This may help to approximate a complex surface by a suitable hidden variable IFS and is proposed to be done in a subsequent work.

ACKNOWLEDGMENTS

This work was partially supported by the Council of Scientific and Industrial Research, India (Grant No. 9/92(160)/98-EMR-I).

REFERENCES

1. B. B. Mandelbrot, D. E. Passoja and A. J. Paullay, "Fractal Character of Fracture Surfaces of Metals," *Nature* **308**, 721–722 (1984).
2. P. Wong, J. Howard and J. Lin, "Surfaces Roughening and the Fractal Nature of Rocks," *Phys. Rev. Lett.* **57**(5), 637–640 (1986).
3. B. B. Nakos and C. Mitsakaki, "On the Fractal Character of Rock Surfaces," *Int. J. Rock Mech. Min. Sci. Geomech. Abstr.* **28**(6), 527–533 (1991).
4. C. S. Pande, L. R. Richards and S. Smith, "Fractal Charcteristics of Fractured Surfaces," *J. Met. Sci. Lett.* **6**, 295–297 (1987).

5. H. Xie, J. Wang and E. Stein, "Direct Fractal Measurement and Multifractal Properties of Fracture Surfaces," *Phys. Lett.* **A242**, 41–50 (1998).
6. D. Anvir, D. Farin and P. Pfeifer, "Molecular Fractal Surfaces," *Nature* **308**, 261–263 (1984).
7. X. C. Jin, S. H. Ong and Jayasooriah, "Fractal Characterization of Kidney Tissue Sections," *IEEE Int. Conf. Eng. Med. Biol. Baltimore,USA* **2**, 1136–1137 (1994).
8. M. F. Barnsley, "Fractal Functions and Interpolations," *Construct. Approx.* **2**, 303–329 (1986).
9. M. F. Barnsley, *Fractals Everywhere* (Academic Press, Orlando, Florida, 1988), Chap. 6, pp. 205–245.
10. M. F. Barnsley, J. Elton, D. P. Hardin and P. R. Massopust, "Hidden Variable Fractal Interpolation Functions," *SIAM J. Math. Anal.* **20**(5), 1218–1242 (1989).
11. P. R. Massopust, "Fractal Surfaces," *J. Math. Anal. Appl.* **151**, 275–290 (1990).
12. J. Feder, *Fractals* (Plenum Press, New York, 1988), Chaps. 13 and 14, pp. 212–243.
13. J. S. Germino and D. P. Hardin, "Fractal Interpolation Surfaces and a Related 2-D Multiresolution Analysis," *J. Math. Anal. Appl.* **176**, 561–586 (1993).
14. J. S. Germino, D. P. Hardin and P. R. Massopust, "Fractal Surfaces, Multiresolution Analyses and Wavelet Transforms," *NATO ASI Series* **F106**, 275–290 (1994).
15. P. R. Massopust, *Fractal Functions, Fractal Surfaces and Wavelets* (Academic Press, 1994), Chap. 5, pp. 135–203.
16. H. Xie and H. Sun, "The Study of Bivariate Fractal Interpolation Functions and Creation of Fractal Interpolated Surfaces," *Fractals* **5**(4), 625–634 (1997).
17. P. R. Massopust, "Vector-valued Fractal Interpolation Functions and Their Box Dimension," *Aequationes Mathematicae* **42**, 1–22 (1991).
18. M. F. Barnsley and A. N. Harrington, "The Calculus of Fractal Interpolation Functions," *J. Approx. Theory* **57**, 14–34 (1991).
19. S. Gibert and P. R. Massopust, "The Exact Hausdorff Dimension for a Class of Fractal Functions," *J. Math. Anal. Appl.* **168**(1), 171–183 (1992).
20. B. B. Mandelbrot, *The Fractal Geometry of Nature* (W. H. Freeman, New York, 1983), p. 365.